New Test Beam Results of 3D and Pad Detectors Constructed with Poly-Crystalline CVD Diamond

M. Reichmann[x,*], A. Alexopoulos[c], M. Artuso[t], F. Bachmair[x], L. Bäni[x], M. Bartosik[c], J. Beacham[m], H. Beck[w], V. Bellini[b], V. Belyaev[l], B. Bentele[s], A. Bes[aa], J-M. Brom[g], M. Bruzzi[d], G. Chiodini[z], D. Chren[r], V. Cindro[i], G. Claus[g], J. Collot[aa], J. Cumalat[s], A. Dabrowski[c], R. D'Alessandro[d], D. Dauvergne[aa], W. de Boer[j], S. Dick[m], C. Dorfer[x], M. Dünser[c], G. Eigen[ad], V. Eremin[f], J. Forneris[o], G.T. Forcolin[v], L. Gallin-Martel[aa], M.L. Gallin-Martel[aa], K.K. Gan[m], M. Gastal[c], C. Giroletti[q], M. Goffe[g], J. Goldstein[q], A. Golubev[h], A. Gorišek[i], E. Grigoriev[h], J. Grosse-Knetter[w], A. Grummer[u], B. Gui[m], M. Guthoff[c], B. Hiti[i], D. Hits[x], M. Hoeferkamp[u], T. Hofmann[c], J. Hosslet[g], J-Y. Hostachy[aa], F. Hügging[a], C. Hutton[q], J. Janssen[a], J. Janssen[z], H. Kagan[m], K. Kanxheri[ab], G. Kasieczka[x], R. Kass[m], M. Kis[e], G. Kramberger[i], S. Kuleshov[h], A. Lacoste[aa], S. Lagomarsino[d], A. Lo Giudice[o], I. López Paz[v], E. Lukosi[y], C. Maazouzi[g], I. Mandic[i], A. Marino[s], C. Mathieu[g], M. Menichelli[ab], M. Mikuž[i], A. Morozzi[ab], J. Moss[ac], R. Mountain[t], A. Oh[v], P. Olivero[o], D. Passeri[ab], H. Pernegger[c], R. Perrino[z], M. Piccini[ab], F. Picollo[o], M. Pomorski[k], R. Potenza[b], A. Quadt[w], F. Rarbi[aa], A. Re[o], S. Roe[c], P.S. Salter[ae], D.A. Sanz Becerra[x], M. Scaringella[d], C.J. Schmidt[e], E. Schioppa[c], S. Schnetzer[n], S. Sciortino[d], A. Scorzoni[ab], S. Seidel[u], L. Servoli[ab], D.S. Smith[m], B. Sopko[r], V. Sopko[r], S. Spagnolo[z], S. Spanier[y], K. Stenson[s], R. Stone[n], B. Stugo[ad], C. Sutera[b], B. Tannenwald[m], M. Traeger[e], D. Tromson[k], W. Trischuk[p], M. Truccato[o], C. Tuve[b], J. Velthuis[q], N. Venturi[c], S. Wagner[s], R. Wallny[x], J.C. Wang[t], J. Weingarten[w], C. Weiss[c], N. Wermes[a], M. Yamouni[aa], M. Zalieckas[ad], M. Zavrtanik[i]

[a] *Universität Bonn, Bonn, Germany,* [b] *INFN/University of Catania, Catania, Italy,* [c] *CERN, Geneva, Switzerland,* [d] *INFN/University of Florence, Florence, Italy,* [e] *GSI, Darmstadt, Germany,* [f] *Ioffe Institute, St. Petersburg, Russia,* [g] *IPHC, Strasbourg, France,* [h] *ITEP, Moscow, Russia,* [i] *Jožef Stefan Institute, Ljubljana, Slovenia,* [j] *Universität Karlsruhe, Karlsruhe, Germany,* [k] *CEA-LIST Technologies Avancees, Saclay, France,* [l] *MEPHI Institute, Moscow, Russia,* [m] *The Ohio State University, Columbus, OH, USA,* [n] *Rutgers University, Piscataway, NJ, USA,* [o] *University of Torino, Torino, Italy,* [p] *University of Toronto, Toronto, ON, Canada,* [q] *University of Bristol, Bristol, UK,* [r] *Czech Technical University, Prague, Czech Republic,* [s] *University of Colorado, Boulder, CO, USA,* [t] *Syracuse University, Syracuse, NY, USA,* [u] *University of New Mexico, Albuquerque, NM, USA,* [v] *University of Manchester, Manchester, UK,* [w] *Universität Göttingen, Göttingen, Germany,* [x] *ETH Zürich, Zürich, Switzerland,* [y] *University of Tennessee, Knoxville, TN, USA,* [z] *INFN-Lecce, Lecce, Italy,* [aa] *LPSC-Grenoble, Grenoble, France,* [ab] *INFN-Perugia, Perugia, Italy,* [ac] *California State University, Sacramento, CA, USA,* [ad] *University of Bergen, Bergen, Norway,* [ae] *University of Oxford, Oxford, UK,*

Abstract

Chemical Vapour Deposition (CVD) diamond is being considered as a material for particle detectors in a harsh radiation environment. This article presents beam test results of 3D pixel detectors fabricated with poly-crystalline CVD diamonds. The cells of the devices had a size of 50 µm × 50 µm with columns 2.6 µm in diameter. The cells were ganged in a 3×2 and 5×1 pattern to match the layouts of the pixel read-out chips currently used in the CMS and ATLAS experiments at the Large Hadron Collider, respectively. In beam tests, using tracks reconstructed with a high precision tracking telescope, both devices achieved tracking efficiencies greater than 97 %. The efficiency of both devices plateaus at a bias voltage of 30 V. Also irradiated poly-crystalline CVD diamond pad detectors were investigated. In high rate beam test with particle fluxes up to 20 MHz/cm^2 and irradiations up to $8 \cdot 10^{15}$ n/cm^2 it was shown that the pulse height of irradiated poly-crystalline CVD diamonds does not depend on flux to the $O(2\,\%)$.

Keywords: Chemical Vapour Deposition, pCVD diamond, diamond detectors, 3D diamond detectors, 3D sensors, radiation tolerant detectors, particle flux

1. Introduction

The radiation levels of the High-Luminosity Large Hadron Collider (HL-LHC) will become a big challenge for the future detectors. By 2028 an instantaneous luminosity of $7.5 \cdot 10^{34}$ cm^{-2} s^{-1} is expected. In this environment the innermost tracking layer at a transverse distance of ~30 mm to the interaction point is expected to be exposed to a total fluence of $2 \cdot 10^{16}$ n$_{eq}$/cm^2 which corresponds to a total dose of the $O(10\,\text{MGy})$ [1]. After such large dose, all detector materials become trap limited with a schubweg below 75 µm. The expected lifetime of the current planar silicon tracking detectors would be about one year in the HL-LHC.

Due to its properties, such as the displacement energy of 42 eV/atom and the band gap of 5.5 eV, the RD42 collaboration is investigating CVD diamond as a possible detector material [2]. In various studies it was shown that compared to analogous silicon detectors, diamond is at a minimum three times more radiation hard [3], collects the charges at least two times faster [4] and conducts heat four times more efficiently [5].

*Corresponding author

By now the technology of diamond detectors is well established in high energy physics. Many high energy physics experiments are already using Beam Condition Monitors or Beam Loss Monitors based on CVD diamonds [6], [7], [8].

The RD42 collaboration is investigating a novel detector design in diamond, namely 3D detectors. The 3D concept reduces the drift distance an electron-hole pair must undergo to reach an electrode below the schubweg of an irradiated sensor without reducing the amount of created electron-hole pairs.

The particle flux of the HL-LHC will also reach a completely new regime. Hence it is important to study diamond detectors at high rates of particles.

2. 3D Pixel Detectors

By placing column-like electrodes inside the detector material, the 3D geometry reduces the drift distance of a charge created by ionising particles compared to a planar device. More details about the working principle can be found in [9], [10]. All devices discussed in this article were constructed with polycrystalline CVD (pCVD) diamond.

2.1. Fabrication

In order to manufacture the electrodes in diamond, columns are fabricated using a 130 fs laser with a wavelength of 800 nm which is used to convert the diamond into a electrically resistive mixture of different carbon phases [11]. By using Spacial Light Modulation (SLM) a column yield of >99 %, a column diameter of 2.6 µm and a resistivity of the columns of the order of $0.1 \sim 1\,\Omega$ cm were achieved [12]. The largest fabricated device had about 4000 3D cells, where one cell consists of four bias electrodes and one readout electrode in the centre.

The detector is constructed by connecting to the bias and readout columns with surface metallisation and bump bonding the sensor to the readout electronics as shown in Figure 1. For the detectors described herein a cell size of 50 µm × 50 µm was chosen. Since the layout of the available readout chips (ROCs) has a different pixel pitch several cells were ganged together.

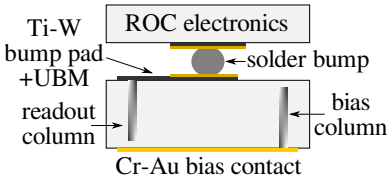

Figure 1: Bump bonding scheme.

2.2. PSI46digV2.1respin readout

The first prototype of a 50 µm × 50 µm 3D pixel detector was connected to the PSI46digV2.1respin ROC [13] with a 3 × 2 cell ganging to match the pixel pitch of 150 µm × 100 µm. The 3D sensors were bump bonded to the ROC at the Nanofabrication Lab at the Princeton University with indium bumps by putting equal height indium columns on both ROC and the sensor and then pressing them together.

The hit efficiency is defined as the percentage of hits in the 3D pixel detector when a particle track traversed the detector. The preliminary beam test results show that, relative to a planar silicon device, the efficiency in the fiducial area was 99.3 % (Figure 2a). This efficiency estimation does not account for non-working 3D cells in this region which can happen due to broken or missing columns or due to metalisation issues. In order to acquire this information further data should be analysed. Nevertheless, a small mismatch between a 3D and a planar device is expected due to regions inside of the detector where the electric field is low [14] and the relatively inefficient columns themselves. Figure 2b shows that the device plateaus at a voltage of 30 V. The preliminary analysis of the pulse height distribution yields a mean value of ~11 ke. The precise pulse height calibration of the ROC is currently being studied.

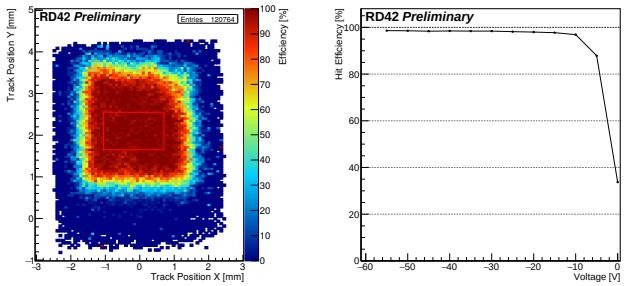

(a) Efficiency map. The red box marks the fiducial area.

(b) Efficiency vs. voltage in the fiducial area.

Figure 2: Hit efficiency results with PSI46digV2.1respin readout.

2.3. FE-I4b readout

The second prototype was connected to the FE-I4b ROC [15] with a 5 × 1 cell ganging due to the ROC pitch of 250 µm × 50 µm. The bump bonding was performed at IFAE-CNM in Barcelona by an adapted process with tin-silver bumps. Using a high resolution beam telescope with a spatial resolution of 3 µm at the device under test the efficiency could be mapped to the spatial coordinates. The analysis yields an efficiency of 97.8 % in the contiguous fiducial area (Figure 3). The lower

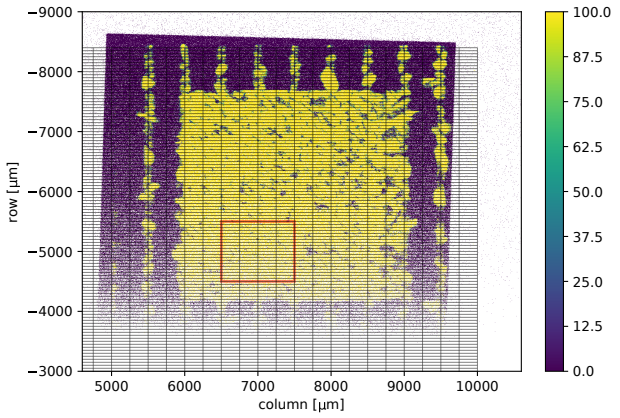

Figure 3: Hit efficiency results with the FE-I4b readout. The red box denotes the fiducial area.

than 99 % efficiency is most likely due to issues with the bump bonding or the metallisation. The preliminary pulse height in the fiducial region was ~15 ke which is consistent with the result of the first prototype considering the different momenta of the incident particles. The precise pulse height calibration for the FE-I4b ROC is in the process of being performed.

3. High Rate Studies

At the HL-LHC particle fluxes will reach the $O\left(\mathrm{GHz/cm^2}\right)$ hence it is very important to understand the effect of the incident particle flux on the signal of all prospective detectors. In order to conduct a high rate study it is necessary to be able to vary the particle flux over a large range. The πM1 beam line at the High Intensity Proton Accelerator (HIPA) at Paul Scherrer Institut (PSI) [16] can provide beams with continuously tunable fluxes from the order of 1 kHz/cm^2 up to 20 MHz/cm^2. The πM1 beam is bunched with a spacing of 19.7 ns. For these studies a π^+ beam with a momentum of 260 MeV/c was chosen in order to reach the highest possible flux [17]. In total 13 pCVD diamonds were measured which were all prepared in the same way.

3.1. Setup

The planar diamond sensors were connected in a pad geometry and prepared as described in [18]. In order to resolve individual particles at high particle rates the sensors were connected to a fast, amplifier with low electronic noise and a rise time of approximately 5 ns. The resulting waveforms were digitised and recorded in a beam telescope setup [18] which provides spatial information of the hits in the diamond detector. Due to the low momentum of the incident particles the spatial resolution of the telescope was of the $O\left(100\,\mu\mathrm{m}\right)$.

3.2. Results

In order to measure the signal behaviour as a function of incident particle flux and irradiation, several rate scans with both polarities of the bias voltage were performed. Figure 4 shows the preliminary results for a pCVD diamond with various fluences up to a maximum particle flux of 20 MHz/cm^2. The sensor was irradiated with fast reactor neutrons in steps up to total fluence of $8 \cdot 10^{15}$ n/cm^2 at the irradiation facilities at the JSI TRIGA reactor in Ljubljana [19]. The mean pulse height of the single rate scans is scaled to 1. The results show that the pulse height is flat with respect to the flux deviating less than 2 % from the mean.

The effect of particle rate on the beam induced current in diamond detectors was also measured. 80 % of the measured diamonds had currents proportional to the flux and a leakage current without a beam of the $O\left(1\,\mathrm{nA}\right)$. The other 20 % show shifting base lines or erratic dark currents [20]. These diamonds are considered problematic and were not analysed for this article.

pCVD diamond has an interior crystal structure where the individual grains have slightly different properties. Therefore the size of the measured signal in pCVD diamond depends also

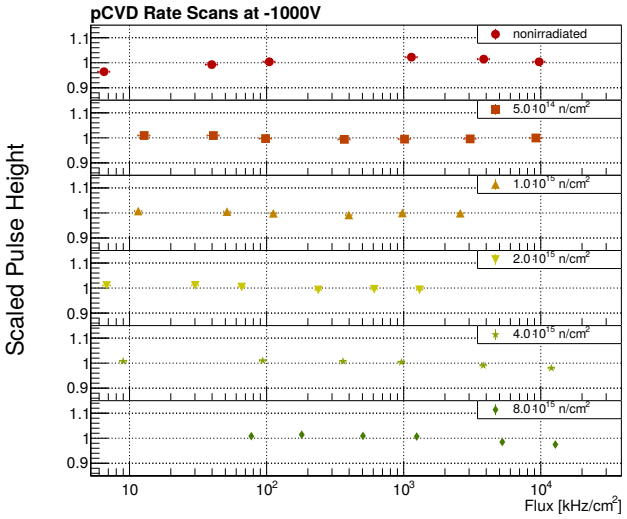

Figure 4: Pulse height versus incident particle flux for a pCVD diamond for various fluences at −1000 V.

on the spatial position as can be seen in Figure 5. A constant fiducial region was used to remove effects of the spatial dependence.

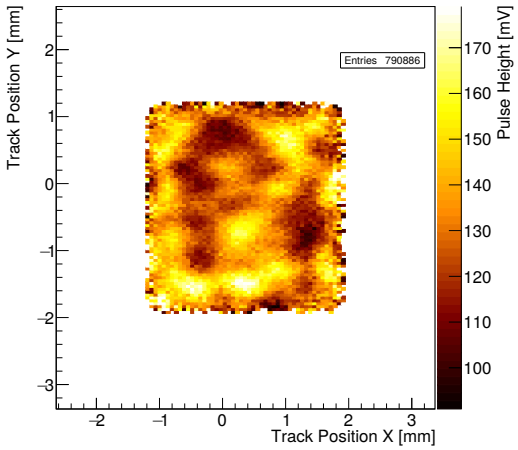

Figure 5: Pulse height map of a pCVD diamond as a function of spatial position.

We also observed a single diamond with a large rate dependence losing 90 % of the signal at the highest rate. After the surface was cleaned and processed with Reactive Ion Etching (RIE), the device was re-metallised. A new measurement showed a deviation of less than 2 % from the mean pulse height. This leads us to the conclusion that this rate effect was due to surface properties and is possible to repair.

4. Conclusion

There is progress in the development of radiation tolerant particle detectors based on pCVD diamonds. The working principle of 3D diamond pixel detectors was proven for cell sizes of 50 µm × 50 µm and column diameters of 2.6 µm. The largest device had a number of 4000 cells and the efficiency of the column drilling process is above 99 %. The first prototypes of

small cell 3D diamond pixel detectors read out more charge than any planar pCVD diamond detector. The measured relative hit efficiency of the 3D pixel detectors reached 99.3 % compared to a planar silicon device.

It was found that irradiated pCVD diamond detectors work reliably and there is no signal variation greater than 2 % up to an incident particle flux of 20 MHz/cm^2. This was shown for a range of irradiations up to a maximum fluence of $8 \cdot 10^{15}$ n/cm^2. The beam induced current of a pCVD diamond is proportional to the flux and the leakage current is of the $\mathcal{O}$(1 nA). It was also demonstrated that it is possible to correct a large rate dependence that occurs in a small fraction of diamonds and is most likely due to surface properties.

Acknowledgements

We want to thank Bert Harrop at the Physics Department of the Princeton University and the team at IFAE for bump bonding our devices.

The research leading to these results received funding from the European Union's Horizon 2020 research and innovation program under grant agreement No. 654168. This work was also partially supported by the Swiss National Science Foundation grant #20FL20_154216, ETH grant 51 15-1, the Swiss Government Excellence Scholarship ESKAS No. 2015.0808, the Royal Society Grant UF120106, the UK Science and Technology Facilities Council Grant ST/P002846/1 and the U.S. Department of Energy through grant DE-SC0010061

References

1. Contardo D, Klute M, Mans J, Silvestris L, Butler J. Technical Proposal for the Phase-II Upgrade of the CMS Detector. Tech. Rep. CERN-LHCC-2015-010. LHCC-P-008. CMS-TDR-15-02; Geneva; 2015. URL: http://cds.cern.ch/record/2020886.
2. Kagan H, et al. (RD42). Development of Diamond Tracking Detectors for High Luminosity Experiments at the LHC, HL-LHC and Beyond. Tech. Rep. CERN-LHCC-2018-015. LHCC-SR-005; CERN; Geneva; 2018. URL: https://cds.cern.ch/record/2320382.
3. de Boer W, et al. Radiation hardness of diamond and silicon sensors compared. *Physica Status Solidi Applied Research* 2007;204:3004–10. doi:10.1002/pssa.200776327. arXiv:0705.0171.
4. Pernegger H, et al. Charge-carrier properties in synthetic single-crystal diamond measured with the transient-current technique. *J Appl Phys* 2005;97(7):73704–1. URL: https://cds.cern.ch/record/909063.
5. Zhao S. Characterization of the electrical properties of polycrystalline diamond films. Ph.D. thesis; The Ohio State University; 1994. URL: http://wwwlib.umi.com/dissertations/fullcit?p9421043.
6. Edwards AJ, et al. Radiation monitoring with diamond sensors in BABAR. *IEEE Transactions on Nuclear Science* 2004;51(4):1808–11. doi:10.1109/TNS.2004.832634.
7. Eusebi R, Wallny R, Tesarek R, Dong P, Sfyrla A, Trischuk W, Schrupp C. A Diamond-Based Beam Condition Monitor for the CDF Experiment. 2006:709 –12. doi:10.1109/NSSMIC.2006.355953.
8. Schaefer D. The ATLAS Diamond Beam Monitor: luminosity Detector on the LHC. Tech. Rep. ATL-INDET-PROC-2015-009; CERN; Geneva; 2015. URL: https://cds.cern.ch/record/2034225.
9. Parker S, Kenney C, Segal J. 3D - A proposed new architecture for solid-state radiation detectors. *Nuclear Instruments and Methods in Physics Research Section A: Accelerators, Spectrometers, Detectors and Associated Equipment* 1997;395(3):328 –43. URL: http://www.sciencedirect.com/science/article/pii/S0168900297006943. doi:https://doi.org/10.1016/S0168-9002(97)00694-3.
10. Oh A, et al. (RD42). A 3D diamond detector for particle tracking. *Nuclear Instruments and Methods in Physics Research Section A: Accelerators, Spectrometers, Detectors and Associated Equipment* 2015;786:97 – 104. URL: http://www.sciencedirect.com/science/article/pii/S0168900215003496. doi:https://doi.org/10.1016/j.nima.2015.03.033.
11. Pimenov SM, et al. Femtosecond laser microstructuring in the bulk of diamond. *Diamond and Related Materials* 2009;18(2):196 –9. URL: http://www.sciencedirect.com/science/article/pii/S0925963508003981. doi:https://doi.org/10.1016/j.diamond.2008.07.014.
12. Sun B, Salter PS, Booth MJ. High conductivity micro-wires in diamond following arbitrary paths. *Applied Physics Letters* 2014;105(23):231105. URL: https://doi.org/10.1063/1.4902998. doi:10.1063/1.4902998. arXiv:https://doi.org/10.1063/1.4902998.
13. Kornmayer A, Müller T, Husemann U. Studies on the response behaviour of pixel detector prototypes at high collision rates for the CMS experiment. 2015. URL: https://cds.cern.ch/record/2264667; presented 04 Dec 2015.
14. Forcolin GT, Oh A, Da Via C. Development and simulation of 3D diamond detectors. 2018. URL: https://cds.cern.ch/record/2636028; presented 2018.
15. Garcia-Sciveres M, et al. The FE-I4 Pixel Readout Integrated Circuit. Tech. Rep. ATL-UPGRADE-PROC-2010-001; CERN; Geneva; 2010. URL: https://cds.cern.ch/record/1231359.
16. HIPA. High Intesity Proton Accelerator at PSI. https://www.psi.ch/rf/hipa; 2017.
17. piM1 beam line. Pion and electron fluxes in piM1. http://aea.web.psi.ch/beam2lines/pim1c.html; 2015.
18. Bachmair F. CVD Diamond Sensors In Detectors For High Energy Physics. Ph.D. thesis; Zurich, ETH; 2016. URL: https://inspirehep.net/record/1503510/files/CERN-THESIS-2016-163.pdf.
19. Snoj L, Žerovnik G, Trkov A. Computational analysis of irradiation facilities at the JSI TRIGA reactor. *Applied Radiation and Isotopes* 2012;70(3):483 –8. URL: http://www.sciencedirect.com/science/article/pii/S0969804311005963. doi:https://doi.org/10.1016/j.apradiso.2011.11.042.
20. Edwards AJ, et al. Radiation monitoring with diamond sensors in BABAR. In: *2003 IEEE Nuclear Science Symposium. Conference Record (IEEE Cat. No.03CH37515)*; vol. 1. 2003:83–86 Vol.1. doi:10.1109/NSSMIC.2003.1352003.